Memoirs of the Faculty of Engineering, Nagoya University
Vol. 38, No. 2 (1986)

LPE GROWTH OF InGaAsP EPITAXIAL LAYERS ON GaAs SUBSTRATES

KAZUMASA HIRAMATSU, ISAMU AKASAKI
and NOBUHIKO SAWAKI

Department of Electronics

(Received October 31, 1986)

Abstract

Effects of various growth conditions on surface morphology and compositional non-uniformity of LPE (liquid phase epitaxy) layers of $In_xGa_{1-x}As_yP_{1-y}$ ($y<0.01$) on (100) GaAs are studied. (1) Growth conditions to obtain a smooth and uniform layer is found from results of change in the surface morphology. (2) The interface instability occurring under an undercooling condition in LPE process is studied by means of analysis of Fourier spectra of the surface morphology. (3) Compositional nonuniformity of InGaAsP LPE layers are investigated by means of the precision X-ray diffractometry. The compositional variation taking place at the initial growth stage during several seconds is found. The variation at the initial stage is analyzed theoretically by "growth lines" on an In-Ga-P phase diagram due to the diffusion-limited growth model by comparison with the experiments. Growth conditions to minimize the compositional variation is proposed.

CONTENTS

1. General Introduction

III-V alloy semiconductors have recently received much attention because epitaxial alloy layers lattice-matched to binary compound substrates such as GaAs and InP can cover a wide range of the band gap and can thus be used to form multilayered heterojunction optoelectronic devices (light emitting diode, laser diode, photodetector, etc.). The alloy system $In_xGa_{1-x}As_yP_{1-y}$ is particularly recognized as an important material in the fabrication of optoelectronic devices because of interest for application of fiber optical communications.

However, important problems have been left unsolved on alloy semiconductors with the range of band gaps of visible light, that is, the problems of immiscibility, compositional non-uniformity, crystal imperfection, control of heterojunction, etc. have not been resolved, and then how to relate between these phenomena and crystal growth mechanism is not also understood.

In this paper, effects of growth conditions on surface morphology and compositional non-uniformity of LPE (liquid phase epitaxy) layers of $In_xGa_{1-x}As_yP_{1-y}$ ($y<0.01$) on (100) GaAs are studied. This quaternary alloy is one of the most promising materials for visible emitting devices because of its direct wide energy gap of about 1.9 eV.

Chapter 2 deals with effects of growth conditions on surface morphology of

InGaAsP LPE layers on (100) GaAs substrates and growth conditions to obtain a smooth and uniform layer is investigated.[1)]

Chapter 3 deals with interface instability occurring under an undercooling condition in LPE process of InGaAsP on GaAs using analysis of Fourier spectra of the surface morphology.[2)]

Chapter 4 deals with effects of various growth conditions on the compositional non-uniformity of InGaAsP LPE layers on GaAs by means of the precision X-ray diffractometry, and the compositional variation taking place at the initial stage is studied.[3)]

Chapter 5 deals with analysis of the compositional variation at the initial stage of the LPE growth by "growth lines" on an In-Ga-P phase diagram using the diffusion-limited growth model.[4)]

2. LPE Growth and Surface Morphology of $In_xGa_{1-x}As_yP_{1-y}$ ($y< 0.01$) on (100) GaAs

2. 1. Introduction

It is important to control surface morphology of the layers since surface morphology affects the perfomance of the devices sevrly. There have been many reports on the surface morphology of homoepitaxial layers such as GaAs/GaAs and InP/InP but only a few on the surface morphology of heteroepitaxial layers such as InGaAsP/InP and InGaAsP/GaAs[5~9)]. It has been thought that surface morphology in the InGaAsP/GaAs system depends on the melt composition,[6,7)] the initial supercooling,[5,7)] the growth temperature[7)], the growth time[5)] and the thermal decomposition of the substrate[8,9)]. A characteristic morphology with localized growth was observed in InGaAsP layers on (100) GaAs substrates,[5)] but the origins of the localized growth were not understood.

This chapter shows the effects of the growth time, the growth temperature and the melt composition on the surface morphology of $In_xGa_{1-x}As_yP_{1-y}$ ($y<0.01$) LPE layers on (100) GaAs substrates to investigate the origin of the localized growth of quaternary alloys and to determine growth conditions required to obtain smooth surfaces.

2. 2. Experimental Procedure

LPE layers were grown by a conventional horizontal sliding-boat technique in a stream of H_2 gas. A mirror polished (100) GaAs wafer doped with Si or Cr was cut into a 6×8 mm die and etched with a 2:1:1 mixture of H_2SO_4:H_2O_2:H_2O for 30 sec. The source melt was prepared from a mixture of InP, GaP and InAs polycrystals and In metal. The Ga concentration in the melt (X_{Ga}^{l}) was varied from 0.86 to 1.04 at%, while P and As concentrations in the melt were fixed at $X_P^{l}=2.80$ at% and and $X_{As}^{l}=0.03$ at%, respectively.

After the source melt had been kept at 800℃ for 80 min, it was cooled at a rate of 0.5℃/min. The source melt was then applied to the substrate at an initial growth temperature of $780℃<T_g^{i}<790℃$. After a growth time of 1 sec to 10 min, the melt was wiped off and the boat was cooled rapidly so that the growth layer would not suffer thermal damage. The growth method adopted was mainly the supercooling (ramp cooling) technique, but step cooling was also used for

comparison. The lattice constants of the quaternary layers were measured by X-ray diffraction, and the lattice mismatch ($\Delta a/a$) ranged from -0.03% to 0.25%, depending on X_{Ga}[1]. The quaternary layer had a band gap of about 1.9 eV (λ_p — 6,500 Å).

The surface morphology was studied by photomicrographs, PL (photoluminescence) images and talystep hight profiles. The layer thicknesses were measured from SEM images of the cleaved faces of the LPE layers.

2. 3. Results

2. 3. 1. Effects of Growth Time

Figure 2.1 shows photomicrographs of the epitaxial layers grown by the supercooling technique for various growth times t_g of 20 sec to 6 min at the initial growth temperature T_g^i of 785℃. The surfaces of the layers grown for $t_g<3$ min (Fig. 2.1 (a)-(c)) have ripples whose structure depends on t_g, whereas smooth mirror-like surfaces appear for $t_g>6$ min (Fig. 2.1 (d)). In Fig. 2.1 (e), the surface morphology formed by the step-cooling technique is also show for comparison. In this, the growth temerature T_g was kept at 785℃. Even if t_g is 10 min, the surface does not become smooth and has wider ripples than those of Fig. 2.1 (a)-(c).

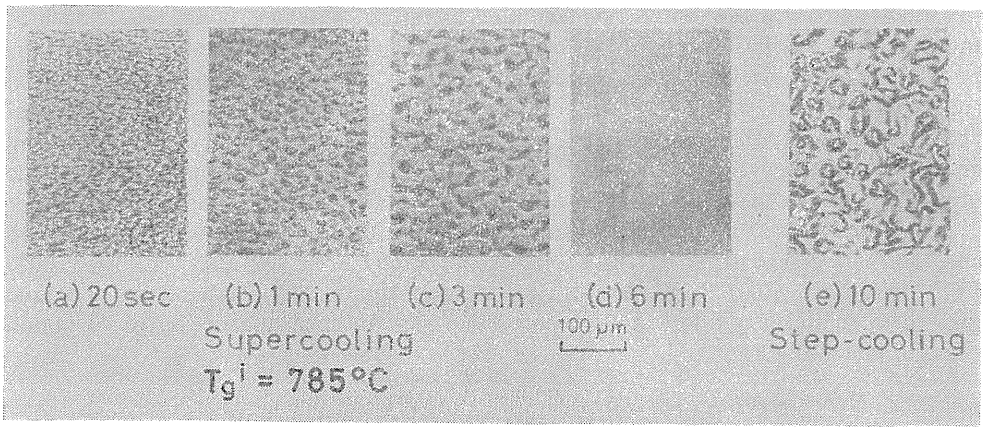

Fig. 2. 1. Photomicrographs of InGaAsP layers for various growth times (a)-(d): by supercooling technique, (e): by step-cooling technique.

Figure 2.2 shows a typical example of the SEM image of (110) cleaved faces along with its schematic illustration. This SEM image shows that the interface between the grown layer and the substrate is not flat, and it has a wavy configuration similar to the rippled surfaces. In addition, the substrate together with the growth region appears on the surface. This indicates that GaAs substrate is partially dissolved into the melt and InGaAsP layer partially grows simultaneously.

The height profile of talystep measurement was used to study the change in the surface morphology. Figure 2.3 shows the profiles of the samples mentioned above. For $t_g=20$ sec, the surface has irregular fine ripples, and for $t_g=1$ min,

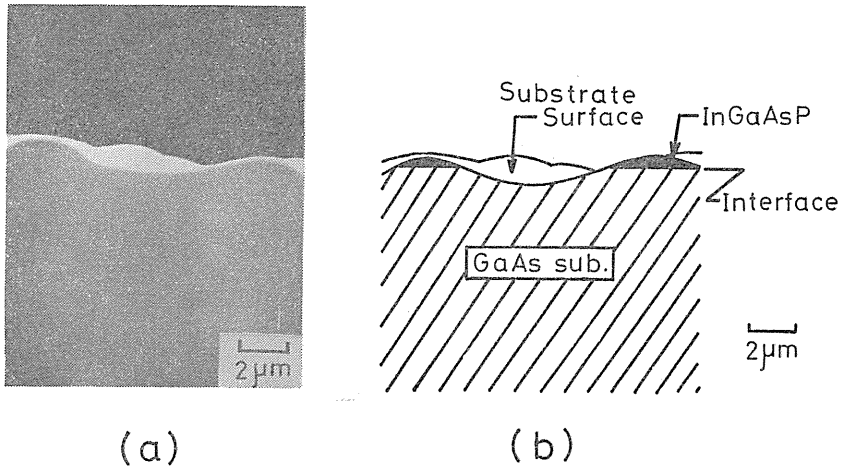

Fig. 2. 2: (110) cleaved face of a sample with rippled surface grown for 1 min at 789°C. (a) SEM image, (b) its schematic illustration.

it is nearly sinusoidal. For t_g=3 min flat planes appear in the sinusoidal surface and for t_g=6 min the surface is completely flat. The width and height of the ripples are defined in Fig. 2. 3. The width increases from 7 to 20 μm with t_g. The height is about 0. 25 μm for t_g<3 min. However, the sample grown by the step cooling technique has a height and width of about 1. 5 and 30 μm, respectively, and both are larger than the supercooling ones. These results suggests that the surface morphology is not determined by the growth time but is related to the temperature during the growth because in the supercooling technique the growth temperature decreases with increasing the growth time.

2. 3. 2. *Effects of Growth Temperature*

Effects of the growth temperature were studied by the supercooling technique at growth time t_g of 1 min. Figure 2. 4 (a)-(d) shows microphotographs of surfaces of the layers grown at various T_g^i of 790 to 782. 5℃ The surfaces for initial growth temperature $T_g^i \geqq 785$℃ have fine ripples whose structure depends also on T_g^i (Fig. 2. 4 (a)-(c)), whereas for $T_g^i \leqq$ 782. 5℃ they are smooth and mirror-like (Fig. 2. 4 (d)). Talystep measurement (Fig. 2. 5) shows that the width of the ripples is increased from 6 to 13 μm by decreasing T_g^i.

Fig. 2. 6 shows the surface morphology as a function of T_g and t_g. The melt

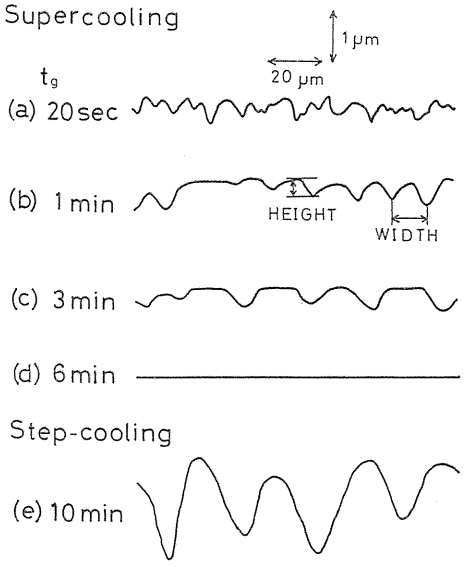

Fig. 2. 3. Talystep height profiles of surfaces of the samples shown in Fig. 2. 1 (a)-(e).

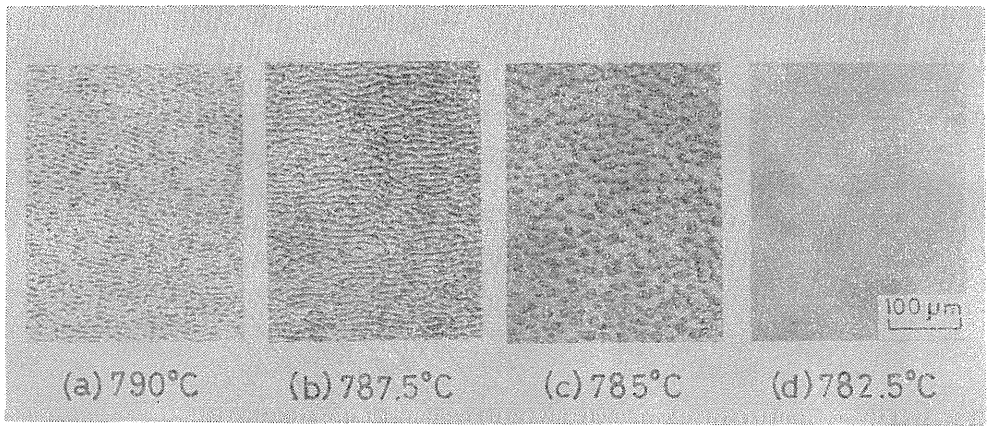

Fig. 2. 4. Photomicrographs of InGaAsP layers for various growth temperatures, grown for 1 min by supercooling technique.

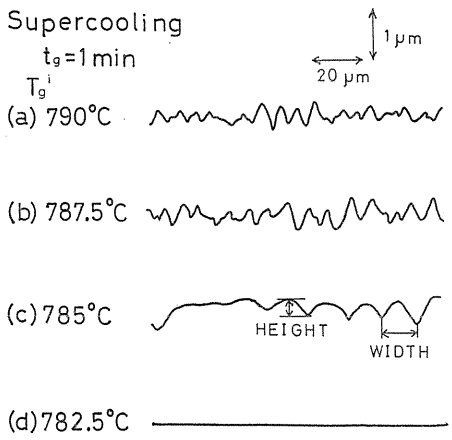

Fig. 2. 5. Talystep height profiles of surfaces of the samples shown in Fig. 2. 4. (a)-(d).

concentrations are X_{In}^{l}=96. 25 at%, X_{Ga}^{l} =0. 92 at%, X_{P}^{l}=2. 80 at% and X_{As}^{l}=0. 03 at%. In the supercooling technique, the temperature is lowered during the growth, as shown by the vertical solid lines in Fig. 2. 6. Considering these growth temperature shifts, we find that a critical temperature T_c separates the surface morphology into two parts of a smooth surface region and a rough surface region. T_c is estimated to be about 784℃ in this experiment. For $T_g > T_c$, the surfaces have ripples and are rough, whereas for $T_g < T_c$, smooth surfaces are obtained. If the vertical lines cross the T_c line, the surface morphology showed an abrupt change. The change in the morphology shows that the morphology depends on the growth temperature rather than the growth time. In the step-cooling technique, the same change in the surface morphology also occurs at the critical temperature, as shown in Fig. 2. 6.

2. 3. 3. Layer Thickness

To investigate the meaning of the critical temperature T_c, we studied the variation of the layer thickness d as a function of the growth time t_g, as shown in Fig. 2. 7. If T_g^i is lower than T_c, the thickness increases as $t_g^{1/2}$. This suggests that diffusion-limited growth plays an important role.[9, 10] If this is the case, the layer thickness is given in a simple formula as a function of growth time for a dilute, semi-infinite solution[10]. According to this model, $t_g^{1/2}$ dependence shows step-cooling-like mechanism. Therefore, it is found that there exists effects of

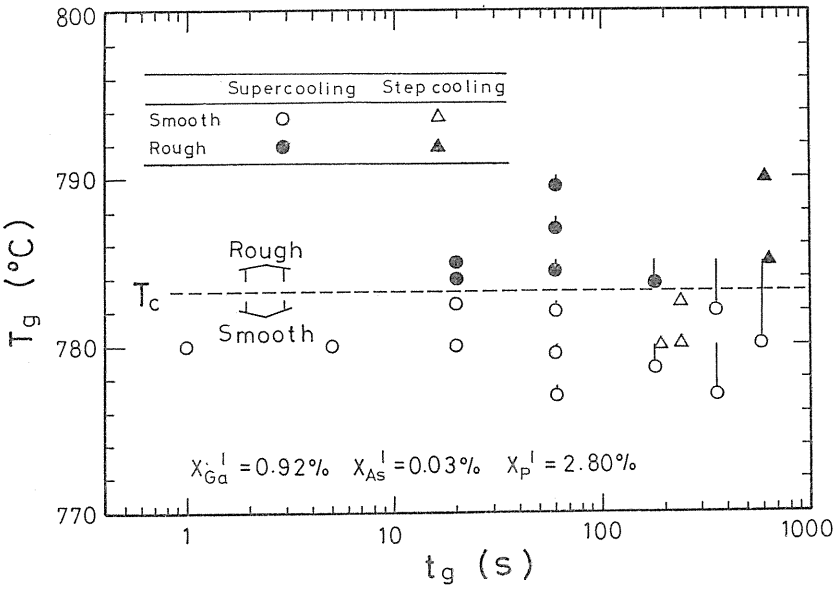

Fig. 2. 6. Variation of surface morphology with growth temperature and growth time.

initial supercooling ΔT on the growth thickness, as described by the formula

$$d \propto t_g^{1/2} \cdot \Delta T$$

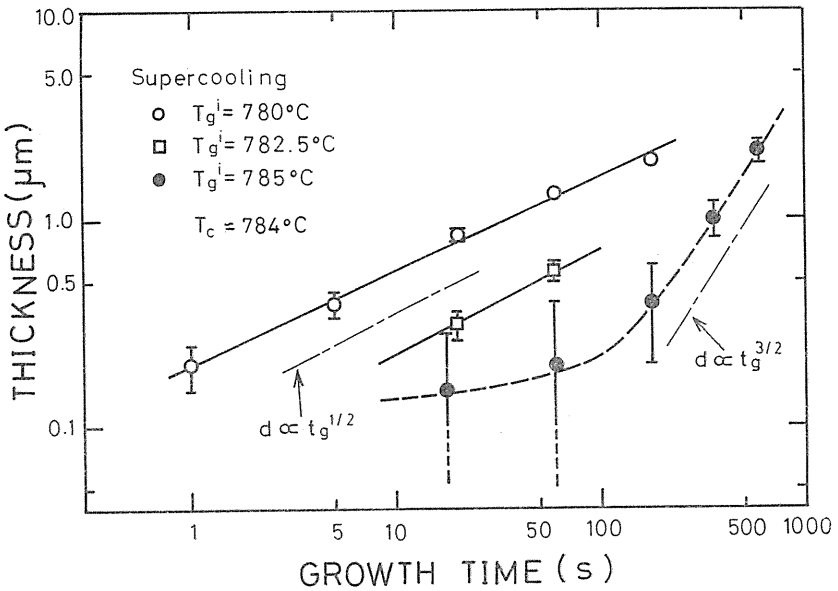

Fig. 2. 7. Layer thickness of InGaAsP for various initial growth temperatures as a function of growth time.

where ΔT is given as a difference between the equilibrium saturation temperature T_s and the initial growth temperature T_g^i, that is, $\Delta T = T_s - T_g^i$. For $T_g^i = 785$℃, the layer thickness increases as $t_g^{3/2}$ for $t_g > 3$ min. If diffusion-limited growth is assumed, the $t_g^{3/2}$ dependence of d suggests that the growth mechanism is equilibrium-cooling-like.[9] Hence, there is no initial supercooling at $T_g^i = 785$℃, in agreement with the fact that $T_g^i = 785$℃ $> T_s$.

Figure 2.8 shows the dependence of the thickness on the growth temperature. By extrapolating the straight lines, the equilibrium saturation temperature is estimated to be $T_s = 784$℃. In the previous section, it was demonstrated that the surface morphology is separated into two groups by T_c (about 784℃). Thus T_c is thought to correspond to the equilibrium saturation temperature T_s. Hence, the change in the surface morphology is determined by the relation betweer T_g and T_s.

Further experiments were made to detremine the degree of the initial supercooling ΔT required to give smooth surfaces. By fixing T_g^i at 782.5℃ and by changing the soaking temperature from 783 to 784℃ (The temperature is thought to be the saturation temperature since it is lower than T_s mentioned above.), several quaternary layers were grown by the supercooling technique, with the growth time of 20 sec. Ripples appeared on the surface for $T_s = 783$℃ ($\Delta T = 0.5$℃), but surfaces for $T_s = 784$℃ ($\Delta T = 1.5$℃) were smooth. Therefore, it was concluded that the smooth surfaces can be obtained if ΔT is as large as 1℃.

2. 3. 4. Effects of Melt Composition

Effects of the melt composition on the surface morphology were also studied. Figure 2.9 shows a map of the surface morphology as a function of T_g and X_{Ga}^l, where X_{As}^l and X_P^l were kept constant at 0.03 at% and 2.80 at%, respectively. The morphology is also separated into two groups of smooth and rough surfaces by the critical temperature. The surfaces are smooth for $T_g < T_c$, but rough for $T_g > T_c$, where T_c increases with increasing X_{Ga}^l. The increase in T_c agrees well with the increase in T_s because T_s increases as the solute concentration increases.

2. 4. Conclusions

The effects of the various growth conditions on the surface morphology of

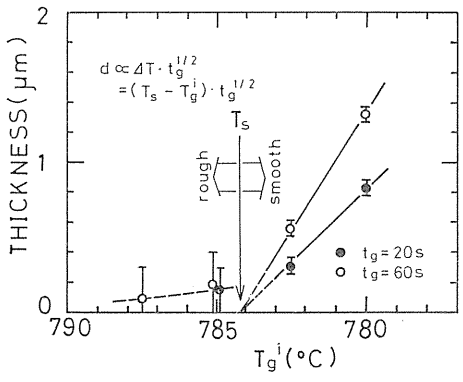

Fig. 2.8. Layer thickness of InGaAsP grown for various growth times as a function of initial growth temperature.

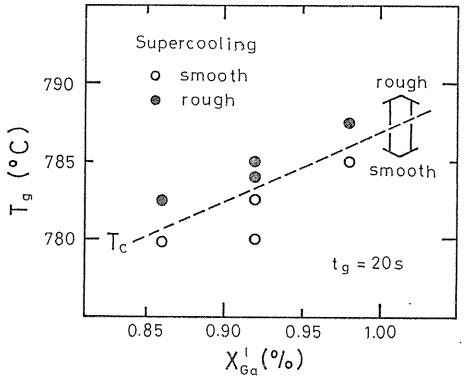

Fig. 2. 9. Surface morphologies as a function of the initial growth temperature and Ga concentration in the melt.

LPE layers of $In_xGa_{1-x}As_yP_{1-y}$ ($y<0.01$) on (100) GaAs were studied. The change in the morphology is determined by the relation between the growth temperature T_g and the equilibrium saturation temperature T_s of the source melt, which is equilibrium with the quaternary solid. The equilibrium temperature of the system was determined by analyzing the growth rate for the qauternary layers. It was found that the partial growth of the quaternary layer takes place on GaAs even at $T_g>T_s$. This is supported by partial melt-back of the substrate. However, when $T_g<T_s$, a smooth surface is obtained if the initial supercooling ΔT is as large as 1℃.

3. Characterization of Morphological Instability in InGaAsP LPE Growth on GaAs by Fourier Analysis

3. 1. Introduction

It has been difficult to obtain a high-quality epitaxial layer of InGaAsP lattice -matched GaAs substrate. This is primary because interfacial instability takes place on the solid-melt (S-M) interface under a condition of a low supersaturation or an undersaturation. Therefore, it is important to investigate the factors which affect the morphology of the LPE layers on GaAs and the mechanism of the interfacial instability.

In some hetero-structures of III-V compoundsa nd their alloys, a smooth interface and/or a smooth surface can not be obtained by LPE growth because of melt-back of the substrate or the layer grown previously. When the melt is brought into contact with the substrate, the dissolution and the growth of the solid take place simultaneously. These phenomena have been reported in various hetero-structures such as InP on InGaAs,[11] InGaP and InGaAsP on GaAs,[1, 5~7] and GaAlSb on GaSb.[12] A surface morphology characteristic to the partial growth of the quaternary layer with the partial melt-back of the substrate was observed in the InGaAsP/GaAs system, as described in chapter 2. The surface morphology is supposed to be related to thermodynamical process due to interrelation among two solid phases (InGaAsP and GaAs) and one melt phase (In-Ga-As-P) on the S-M interface. There are few investigations concerning the interfacial instability in the hetero-epitaxial growth, and so its mechanism is not well known.

In this chapter using a new method for characterization, Fourier analysis, the surface morphology in the InGaAsP LPE growth on (100) GaAs substrate is studied in relation to the growth conditions. Furthermore, the mechanism of the instability is investigated in the light of the theory of the interfacial instability.

3. 2. Experimental Procedure

LPE growth of $In_xGa_{1-x}As_yP_{1-y}$ ($y<0.01$) was carried out on an (100) GaAs substrate using a step-cooling technique. The solute concentrations in In melt were fixed at $X_{Ga}^{l}=0.92$ at%, $X_{As}^{l}=0.03$ at% and $X_{P}^{l}=2.80$ at%. After the melt had been kept at 800℃ for 80 min, it was cooled down to a growth temperature T_g and touched with the substrate at a growth time t_g.

The surface morphology depends strongly on the supercooling ΔT, which is defined as the difference between the equilibrium saturation temperature T_s and T_g. If ΔT is larger than 1℃, a mirror-like smooth surface is obtained, while if ΔT is less than 1℃ or minus, the S-M interface is thermodynamically unstable and

the surface becomes rough because of the partial melt-back of the substrate. It is important, therefore, to estimate the magnitude of ΔT exactly in order to investigate the origin of the rough surface in the hetero-structure.

In this chapter. in order to study the interfacial instability in the hetero-structure the crystal growth has been carried out at higher temperatures than T_s, i. e. under a condition of undersaturation ($\Delta T = T_s - T_g < 0$℃). The value of T_s has been estimated to be about 784℃ for the melt used from the relation between the growth rate and the growth temperature obtained from the experimental results, as described in Chapter 2.

3. 3. Characterization of Surface Morphology by Fourier Analysis

3. 3. 1. Method of the Analysis

Figure 3. 1 shows photomicrographs of the surfaces grown by the step-cooling technique for various growth times t_g of 20 sec to 6 min. T_g was chosen as 786℃ to fix the supercooling ΔT of -2℃ Since ΔT is minus, serious melt-back occurs at the initial growth stage, and so peculiar fine ripples are seen on the surfaces. To investigate the interfacial instability in detail the change in the surface morphology was studied by using Fourier spectral analysis, which enabled us to characterize the surface morphology quantitatively. A talystep height profiler and a signal analyser were used to measure the surface morphology. For the apparatus used, the accuracy in the vertical and lateral direction was about 0. 005 μm and 0. 2 μm, respectively.

Figure 3. 2 shows typical traces for the height profiles obtained by the talystep measurement for the surfaces of the samples as shown in Fig. 3. 1. As t_g is varied from 20 sec to 6 min, the wavelength and the height of the rippled structure are increased. The analog data as in Fig. 3. 2 were converted into the digital ones by a D/A converter, and fast Fourier transformation (FFT) was carried out using the signal analyser, The power Fourier spectra obtained by the FFT are shown in Fig. 3. 3 (a)-(d) as a function of the wave number k, which is defined as

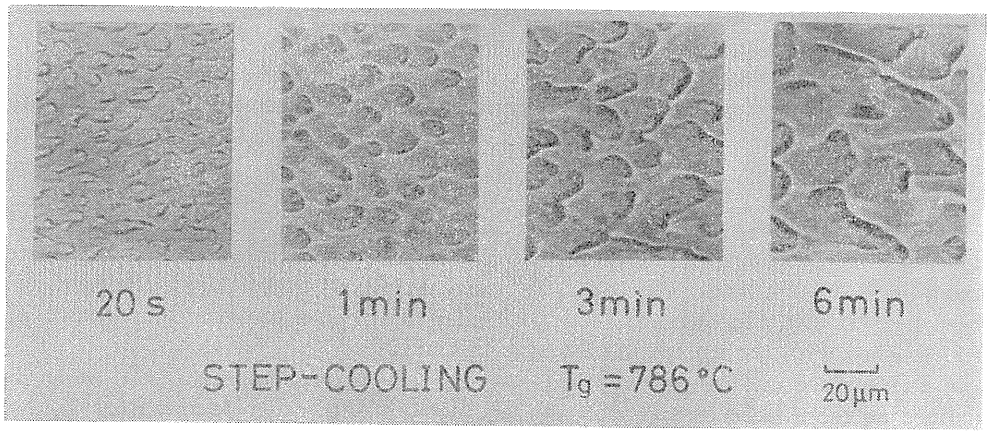

Fig. 3. 1. Photomicrographs of LPE layers grown on (100) GaAs substrates for various growth times.

the reciprocal of the wavelength. The sampling length along the surface was 2.4 mm and the number of the sampling data was 3,072 for one FFT. As is shown in Fig. 3.3, the Fourier spectra are distributed in some range of the wave number but have strong peaks near the center. Therefore, for the convenience of the characterization, we have used Gaussian approximatively to express the spectrum, A typical example of the approxmiate Gaussian distribution is shown in Fig. 3.3 (c). By using a method of least squares the average value $\bar{k}$ and the standard deviation s can be calculated. Here, $\bar{k}$

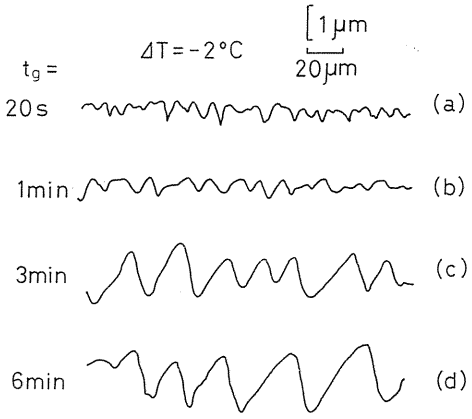

Fig. 3.2. Talystep height profiles of surfaces shown in Fig. 3.1.

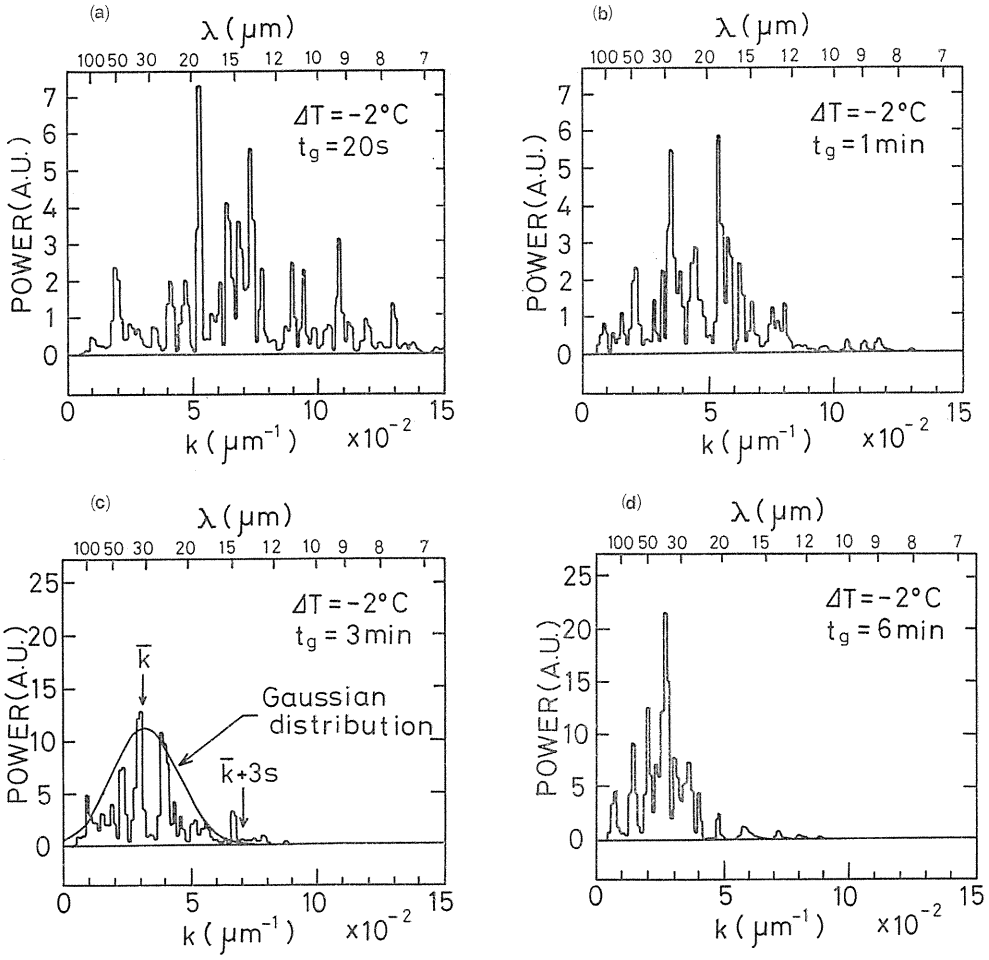

Fig. 3.3. Power Fourier spectra of the surface morphology shown in Fig. 3.2. (a)-(d).

means a typical wave number in the surface morphology. The value of $\bar{k}+3s$ corresponds to a cutoff wave number, that is, a wave with a wave number larger than $\bar{k}+3s$ might not exist on the surface.

In order to check the reliability of this method, FFT was carried out for the various numbers of the sampling data. Figure 3.4 shows $\bar{k}$ and s as a function of the number of the sampling data. If the data number is 1,024, the values of $\bar{k}$ and s are scattered, but if the number of the data is larger than 3,072, the values of $\bar{k}$ and s are independent of the number of the sampling data. In the following, the analysis will be done by using 3,072 points.

3. 3. 2. Effects of the Growth Time

In Fig. 3.5, the variation of the power Fourier spectra deduced from the deta as shown in Fig. 3.3 are reproduced by using Gaussian distributions for various growth times t_g of 20 sec to 10 min at a constant supercooling ΔT of -2℃. For a short growth time less than 1 min, although the maximum of the distribution is relatively small, the standard deviation s is large, i. e., the wave length is distributed over the wide range between 8 and 80μm. These facts suggest that rippled structure with random wave numbers including large ones is formed by the intensive melt-back of the substrates at the initial stage. As the growth time increases, waves with large wave numbers are less prominent, but those with small wave numblers become predominant.

In order to investigate the spectra quantitatively, the variations of $\bar{k}$, $\bar{k}+3s$ and total power $T.P.$ are plotted as a function of the growth time, where $T.P.$ is defined as an area of the Gaussian distribution function and it means the square of the amplitude of the wave according to the Parseval's equality in Fourier transformation. As is shown in Fig. 3.6 (a), $\bar{k}$ and $\bar{k}+3s$ decrease in proportion to $t_g^{-1/3}$. Therefore, the ratio of $\bar{k}$ and $\bar{k}+3s$ is a constant independent of the growth time, i. e., $(\bar{k}+3s)/\bar{k}$ is about 2.0. Figure 3.6(b) shows that $T.P.$ increases with the growth time in proportion to $t_g^{2/3}$, i. e., the amplitude of the wave on

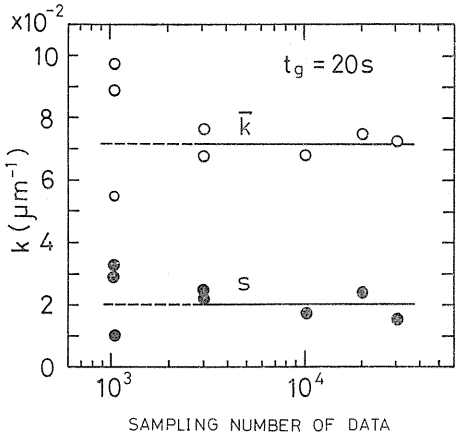

Fig. 3. 4. The average wave number $\bar{k}$ and the standard deviation s as a function of the number of the sampling data used in one FFT.

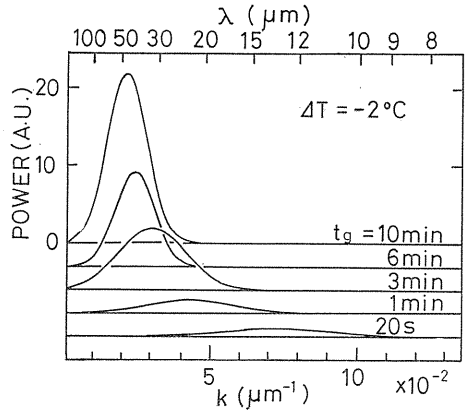

Fig. 3. 5. Power Fourier spectra expressed approximatively by Gaussian distribution as a function for various growth times.

the surface increases as $t_g^{1/3}$. Thus some of the grains widely distributed at the initial stage disappear, and others grow and incorporate into larger clusters, as already shown in Fig 3. 1.

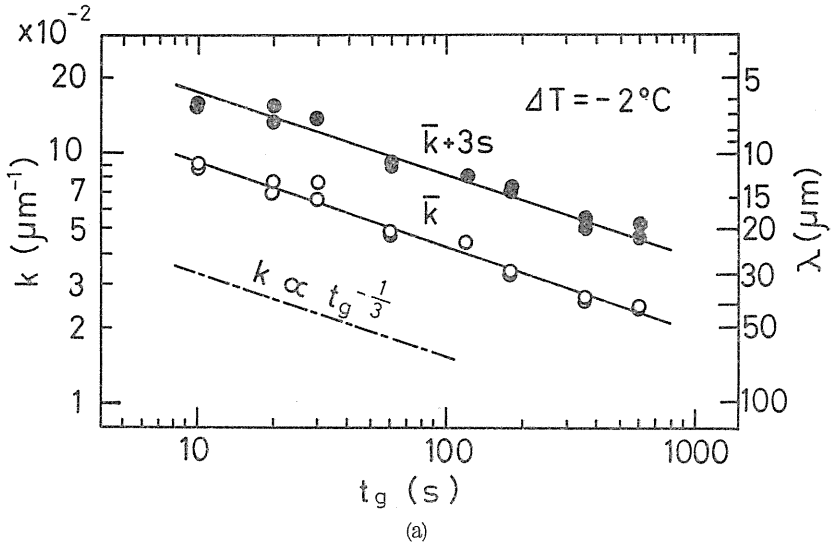

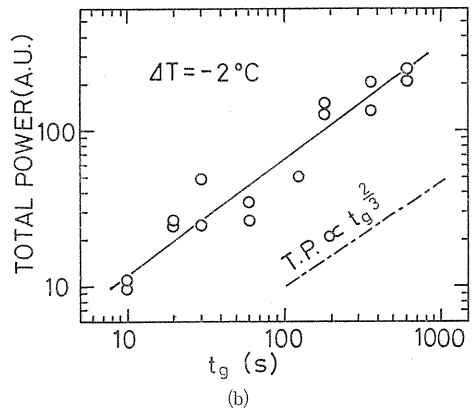

Fig. 3. 6. (a) The average wave number $\bar{k}$ and the cutoff $\bar{k}+3s$, and (b) the total power $T.P.$ as a function of the growth time t_g.

3. 4. Discussion

The growth process of grains known as the Ostwald ripening was investigated theoreticallly by Lifshitz[13] and Wagner.[14] This process is concerned with precipitation of grains in a melt phase, which is caused by the motive force to decrease the interfacial free energy on the solid-melt interface. In this, some grains grow but are later dissolved, and others increase in size and incorporate further grains. This agrees well with the phenomena observed in the present InGaAsP/GaAs system, i. e., the quaternary grains on the hetero-interface grow into larger clusters with time, as shown in Fig. 3. 1.

The theory of the Ostwald growth process gives the distribution function of the grain size as a function of the grain radius and the growth time.[13] According to the formula given by Lifshitz[13] and Wagner,[14] in the diffusion-limited case

the average grain radius $\bar{r}$ depends on time t_g as

$$\bar{r} \propto t_g^{1/3}.$$

Since the grain radius corresponps to the reciprocal of the wave number k, this formula agrees with the experimental result i. e. $\bar{k} \propto t_g^{-1/3}$. As described in the previous section, the amplitude of the wave increases as $t_g^{1/3}$ since the total power $T.P.$ varied as $t_g^{2/3}$. This shows that the time dependence of the grain size in the vertical direction as well as in the lateral one agrees well with the formula of Lifshitz and Wagner. Furthermore, the theoretical grain radius is distributed in some range with a peak near the center, and then the distribution function is independent of time. This is in agreement with the present result that the rario of the average wave number $\bar{k}$ and the cutoff $\bar{k}+3s$ in the Gaussian distribution is a constant independent of time.

The agreement between the theory and experiments suggests that the Ostwald process occurs on the solid-melt interface. Therefore, the mechanism of the interfacial instability in the InGaAsP/GaAs system is attributed to the diffusion of solute atoms along the interface to decrease the interfacial free energy which is related to the interfacial free energy based on the grain size.

3. 5. Conclusion

The interfacial instability which occurred on the hetero-interfaces and surfaces of $In_xGa_{1-x}As_yP_{1-y}$ ($y<0.01$) LPE layers on (100) GaAs substrates was studied using Fourier analysis of the surface morphology. This method enabled us to characterize the wave number distribution of the surface morphology in detail especially with rippled structure. It was found that the wave number is distributed in some range with stronger peaks near the center. The average wave number depends on time as $t_g^{-1/3}$, and its amplitude depends on time as $t_g^{1/3}$. In the light of the interfacial instability theory of the Ostwald growth process, the instability in the hetero-structure was confirmed to be attributed to the diffusion mechanism of the solute to decrease the interfacial free energy along the solid-melt interface.

4. Compositional Non-uniformity of InGaAsP/GaAs LPE Layer by Precision X-ray diffractometry

4. 1. Introduction

The quaternary III-V alloy InGaAsP grown on GaAs has received much attention as a material for visible lasers. In the device application of the alloy, one of the most important properties is the compositional uniformity. In all alloys, however, the compositional non-uniformity may occur. This nonuniformity is much serious problem than the non-stoichiometry in the alloys. Thus, it is strongly desirable to establish the method for measuring the compositional non-uniformity for each alloy. A double crystal X-ray diffractometry makes it possible to study the alloy composition precisely by measuring the lattice constant. In addition, the lattice mismatch in the direction perpendicular as well as parallel to the hetero-interface can be estimated from asymmetric reflections of X-ray.

Several authors studied the compositional non-uniformity of InGaAsP on

InP using the double crystal X-ray diffractometry, and reported a compositional variation,[15,16] which was characteristic of short time growth (less than several seconds).[16] This variation was supposed to be attributed to non-diffusion-limited process such as a convection current due to a motion of a substrate or attachment kinetics of solute atoms.[16] But the details are not well uderstood, and it is desirable to study the effects of the growth conditions especially at short time growth on compositional non-uniformity.

In this chapter the compositional non-uniformity in InGaAsP (100) GaAs LPE layers which were measured using the high resolusion double crystal X-ray diffractometry by (511) asymmetric reflection. The compositional variation is investigated in relation to the various growth conditions such as the lattice mismatch, the initial supersaturation, the temperature fluctuation, and phosphorus adhesion to GaAs. The lattice deformation of the layers due to the lattice mismatch is also shown.

4. 2. Experimental Procedure

Epitaxial layers of $In_xGa_{1-x}As_yP_{1-y}$ ($y<0.01$) were grown on (100) GaAs by supercooling technique. Solute concentrations in In melt were X_{Ga}^l of 0.86 to 1.04 at%, X_{As}^l of 0.03 at% and X_P^l of 2.80 at%. After the melt was kept at 800℃, it was cooled at a rate of 0.5℃/min and touched with the substrate at the growth temperature T_g of 776 to 786℃. The initial supersaturation ΔT was determined as a difference in T_g and T_s (equilibrium saturation temperature). The layer thicknesses obtained were 1−2 μm.

X-ray double crystal rocking curves (called XRC's hereafter) were measured for two arrangements (A and B settings) in (511) asymmetric reflection of CuKα_1 radiation as well as (400) symmetric one.[17] The typical examples of the XRC's are shown in Fig. 4. 1. The half widths of the (511) A and (511) B peaks are about a half of (400) one. Furthermore, the XRC's for the layers in the (511) reflections exhibit two peaks ((i) and (ii)), suggesting that there is compositional non-uniformity in the epitaxial layer. In this work the (511) reflections are studied in detail.

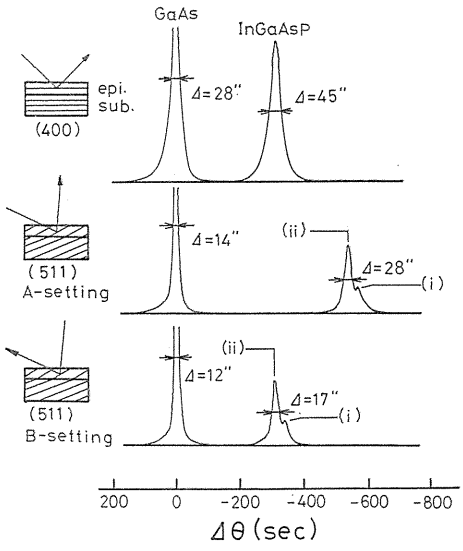

Fig. 4. 1 X-ray rocking curves of InGaAsP/GaAs for the (400), (511)A and (511) B setting reflections. The layer was grown at T_g of 780°C for 3 min by supercooling technique.

4. 3. Results

4. 3. 1. Effects of Lattice Mismatch

In order to study effects of the lattice mismatch, X_{Ga}^l was varied. Figure 4. 2 shows the XRC's of asymmetric (511)A reflection for various Ga concentration

from 0.86 to 1.04 at%, while ΔT was fixed at 4.0℃ and t_g was fixed at 2 min. Smooth mirror-like surfaces were obtained under these conditions. All XRC's of the layers are composed of two peaks ((i) (ii)) and the difference in the reflection angle between both peaks is almost independent of Ga concentration. To investigate the origin of this compositional non-uniformity, the (511)A XRC's were measured successively by repeating step-etching of the epilayer. The results are shown in Fig. 4.3, which shows that the lattice constant varies during growth from the peak (i) to (ii) along the thickness. The growth time to form the initial layer for the peak (i) is estimated at about 5 sec from the growth rate.

The lattice deformation of the layer due to the lattice mismatch was calculated from the XRC's of the (511)A and (511)B settings.[15,17] Fig. 4.4 shows the results. The vertical axes are the lattice mismatch and In atomic fraction x, respectively. Solid circles and open circles stand for the values obtained from the peak (i) and (ii), respectively. Epilayers are tetragonally deformed, i. e., the normal lattice mismatch $(\Delta a/a)_\perp$ is as large as 4×10^{-3} while the lateral one $(\Delta a/a)_\parallel$ is less than 1×10^{-4} for both peaks. It is also shown that the compositional variation from the peak (i) to (ii) is independent of the lattice mismatch.

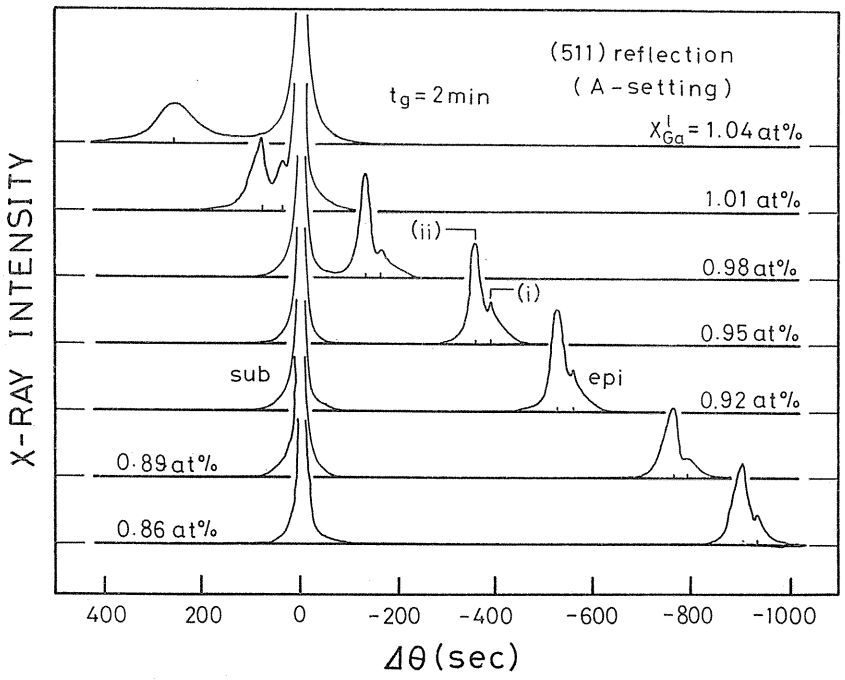

Fig. 4.2. X-ray rocking curves using the (511)A asymmetric reflection for InGaAsP on (100) GaAs for the various Ga concentration in the melt.

4. 3. 2. Effects of Initial Supersaturation

The initial supersaturation ΔT was varied from 2 to 12℃, while the solute concentrations in the melt were fixed at $X_{Ga}{}^l$ of 0.95 at%, $X_{As}{}^l$ of 0.03 at% and $X_P{}^l$ of 2.80 at% so that the equilibrium saturation temperature T_s was 788℃. The

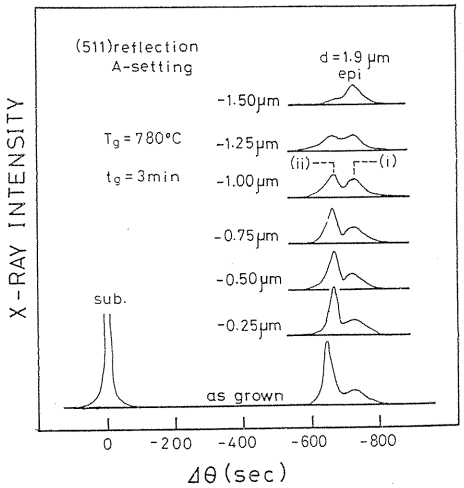

Fig. 4. 3 X-ray rocking curves of the epilayer as-grown and after successive etching.

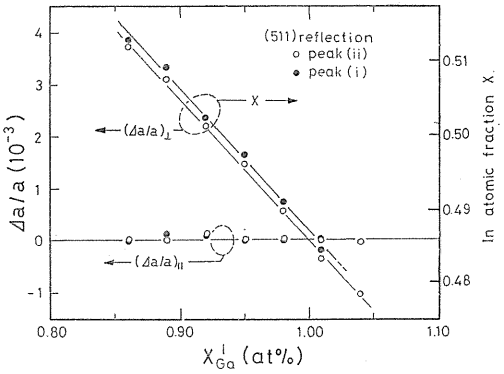

Fig. 4. 4. Lattice mismatch and In atomic fraction as functions of Ga concentration for the peaks (i) and (ii).

growth time was 2 min and the layer thickness was about 2 μm. As seen in Fig. 4. 5, all XRC's of the layers are also resolved into two peaks ((i) and (ii)) except ΔT of 2℃. Fig. 4. 6 shows the normal and lateral mismatches and its In atomi fraction x for the peaks (i) and (ii) as a function of ΔT. The difference in composition between the peaks (i) and (ii) increases by increasing ΔT.

It is therefore concluded that the compositional nonuniformity at the initial

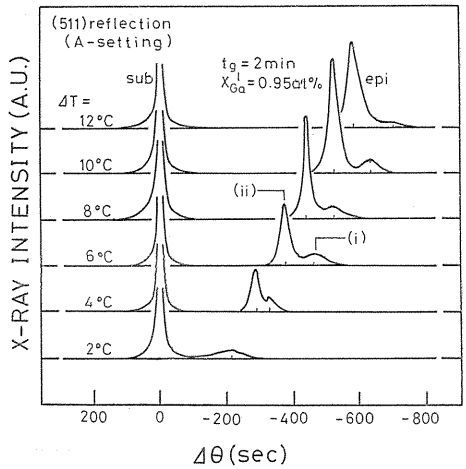

Fig. 4. 5. X-ray rocking curves in the epilayers for the various initial supercooling.

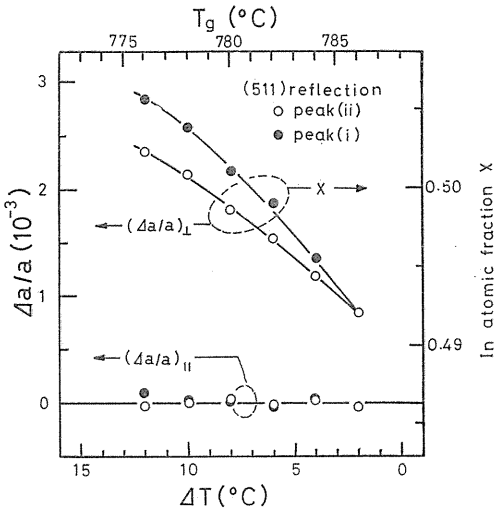

Fig. 4. 6. Lattice mismatch and In atomic fraction as functions of initial supercooling for the peaks (i) and (ii).

stage of the growth strongly depends on ΔT. Therefore, in order to minimize compositional nonuniformity, the initial supersaturation should be as small as possible.

4. 3. 3. Other Effects

The effects of the temperature shift during the growth were studied by measuring the XRC's of the layers grown by the step-cooling technique for comparison. It was found that these XRC's had two peaks and agreed well with those for the supercooling one. This suggests that the compositional variation is not caused by the temperature variation.

The phosphorus molecules vaporized from the source melt adhere to the GaAs substrate before growth.[8,9] This might change the alloy composition at the initial stage of the growth. We compared the XRC's of the layers grown on the substrate with and without the etching process using undersaturated Ga melt of As solute before growth, where the etched layer thickness was about 5 μm. The XRC's for the both cases agreed with each other. Thus, the effect of the adhesion of P atoms can be neglected.

4. 4. Conclusion

The effects of the growth conditions on the compositional non-uniformity of InGaAsP/(100) GaAs were studied by the precision X-ray measurement. It was found that the compositional variation at the initial growth stage is mainly due to the initial supersaturation and that the larger compositional variation is caused by the larger supersaturation.

5. Analysis of Compositional Variation at Initial Growth Stage in LPE of InGaAsP/GaAs

5. 1. Introduction

In the liquid phase epitaxy of InGaAsP on GaAs, the solid composition and the thickness of the layer grown at short time attract much attention because thin epitaxial layers are to be used for the practical applications. Non-uniformity in the solid composition of alloys such as AlGaAs/GaAs,[18,19] InGaAsP/InP,[16,20] and InGaAsP/GaAs[3] have been studied. Experimentally, the compositional variations that occur at the initial growth stage (less than a few seconds) of the LPE has been found using precision X-ray measurements in InGaAsP/InP system[16] and in InGaAsP/GaAs system.[3] In the previous chapter 4, we indicated that the compositional variations depend on the supersaturation. However, there have been only a few reports studying the initial transient phenomena of the compositional variations in the LPE growth.

For LPE growth of ternary or quaternary compounds, the theoretical analysis is much complicated due to the many components in the melt (one solvent and more than two solutes). In fact, the solid composition is affected by various diffusion coefficients of the solutes. To solve this problem, we have to consider the diffusion process of solute atoms and the phase diagram. The latter gives the relation between the melt and solid compositions. The analyses have been made for AlGaAs/GaAs,[18,19] and for InGaAsP/InP[13]. In these simulations, the solute

concentrations were assumed to be in equilibritm with the solid phase at the interface, and the diffusion equations for each solute were solved numerically for the diffusion limited process. However, the initial transient process in the LPE growth are remained unsolved.

The variations of the solid composition and the growth rate were described by the growth line (the crystallzation path) on the phase diahram.[18] In this chapter, the initial transient phenomena on the variation of the solid composition and the growth rate in the LPE growth of $In_xGa_{1-x}As_yP_{1-y}$ ($y<0.01$) is studied in detail by using the growth lines on the phase diagram on In-Ga-P system based on the diffusion limited process by adopting the diffusion coefficients, D_{Ga} and D_P. The experimental variations of the solid composition measured by the precision X-ray diffractometry are compared with the theoretical results.

5. 2. Theoretical Analysis

The growth of III-V semiconductor alloys for the LPE growth have been studied for the diffusion limited growth model by many authors. They have adopted several assumptions: (1) no nucleation within the melt. (2) very fast interface attachment kinetics, (3) no convection. (4) no diffusion in the solid, and (5) a semi-infinite melt.[18] These assumptions will be adopted in the following calculations. The procedure is similar to Crossley and Small,[19] and Ijuin and Gonda.[18]

The calculations will be made for the In-Ga-P ternary phase excluding As because the solid composition y of the layer grown is less than 0.01. Therefore we consider the solid composition x (i. e. molar fraction of InP) for the compositioal variation of $In_xGa_{1-x}P$. The one-dimensional diffusion equations in In melt are given for each component by

$$\frac{\partial X_j^1}{\partial t}=D_j\frac{\partial^2 X_j^1}{\partial z^2} \quad (j=Ga,\ P) \tag{5.1}$$

where D_j is the diffusion coefficient $X_j^1(z, t)$ is the concentration of the component j in the melt, z is the distance from the growing interface, and t is time. By neglecting the diffusion in the solid, the mass conservation of the solute atoms between the melt and the solid gives the growth rate expression:

$$v(t)=\frac{D_{Ga}(\partial X_{Ga}^1/\partial z)_{z=0}}{(1-x)r/2-X_{Ga}^1(0,\ t)}$$

$$=\frac{D_P(\partial X_P^1/\partial z)_{z=0}}{r/2-X_P^1(0,\ t)} \tag{5.2}$$

where r is the ratio of the volume per single atom in the melt to that in the solid and is nearly equal to unity. The corresponding thickness d of the grown layer is given by

$$d=\int_0^t v(t)\mathrm{d}t. \tag{5.3}$$

Since the solid phase should be in equilibrium with the melt phase at the growing interface, we use the phase diagram of th In-Ga-P system to obtain the relation between the solid and melt compositions. The liquidus and solidus iso-

therms are calculated for the regular solution phase equilibrium model by Illegems and Panish for the LPE growth.[21] Well-accepted thermodynamic parameters are used in the calculation.[22] In addition to their models, the effects of strain in the epitaxial layer due to lattice-mismatch with the substrate are taken into account. The mismatch strain energy is included in the total excess free energy G_{tot} as[23]

$$G_{tot}=G_e+G_{st} \tag{5.4}$$

where G_e is the excess free energy due to the melt-solid phase transition and G_{st} is the elastic strain energy caused by the lattice-mismatch.

As mentioned above, the variation of the solid composition is described by a growth line which moves on the phase diagram as a function of the growth time. In practice, the growth line is given by Eq. (5.2). In order to obtain the values of $X_i^l(z, t)$ and x in Eq. (5.2), we must solve simultaneously the diffusion equations (5.1) and the equilibrium equations.[19] Eq. (5.1) are replaced by difference equations, which can be solved numerically.[19] In the following, the growth lines will be calculated for the parameters such as the supercooling ΔT, the ratio D_{Ga}/D_P, and the cooling rate $C.R.$, and hence the solid composition and the layer thickness will be given as a function of the growth time. The values of D_{Ga} and D_P in In-Ga-P melt are not well known. Therefore, they were treated as adjustable parameters.

5. 3. *Theoretical Results*

The growth lines on the In-Ga-P phase diagram calculated for the various $C.R.$'s are shown in Fig. 5. 1. Here, we dealt with the case of no initial supersaturation ($\Delta T=0$℃), i. e. equilibrium-cooling technique. The ratio D_{Ga}/D_P was fixed at 0. 56. The initial concentrations of Ga and P in the melt were chosen as $X_{Ga,0}^l$ of 0. 95 at% and $X_{P,0}^l$ of 2. 80 at%, corresponding to the initial melt prepared in the experiments. By increasing the $C.R.$, the growth line approaches that given by the simpler equation:[18]

$$\frac{D_{Ga}(X_{Ga}^l(0, t)-X_{Ga,0}^l)}{D_P(X_P^l(0, t)-X_{P,0}^l)}=\frac{(1-x)r/2-X_{Ga}^l(0, t)}{r/2-X_P^l(0, t)} \tag{5.5}$$

instead of Eq. (5.2). This growth line (called ultimate growth line hereafter) is shown in the line (u) in Fig. 5. 1. Thus, it is concluded that the variation of the solid composition is affected by the cooling rate and hence the growth rate.

Figure 5. 2 shows the ultimate growth lines calculated for the various values of D_{Ga}/D_P from 0. 4 to 1. 2. Here, D_P was taken 2.3×10^{-4} cm²/s. The initial solute concentrations $X_{Ga,0}$ and $X_{P,0}$ were fixed at 0. 95 at% and 2. 80 at%, respectively. It is shown that the ultimate growth line depends on the diffusion coefficient ratio. Furthermore, it was confirmed that when $D_{Ga}=D_P$, the growth lines are the same for different cooling rates. Thus, the ratio D_{Ga}/D_P has a remarkable influence on the solid composition of the InGaP.

To investigate the effects of the supersaturation, the growth lines were calculated for the various ΔT's from 6 to 12℃ for (1) step-cooling ($C.R.=0$℃/min) and (2) supercooling ($C.R.=0.5$℃/min). The results are shown in Figure 5. 3, where $D_{Ga}/D_P=0.56$ and $D_P=2.3\times10^{-4}$cm²/s. The starting points of the growth lines correspond to the solute concentrations which are determined along the ultimate

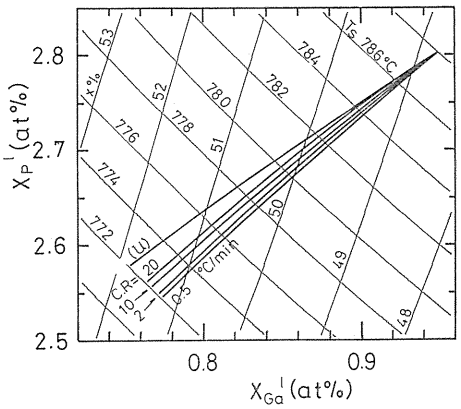

Fig. 5. 1. Growth lines calculated for equilibrium-cooling process at various cooling rates.

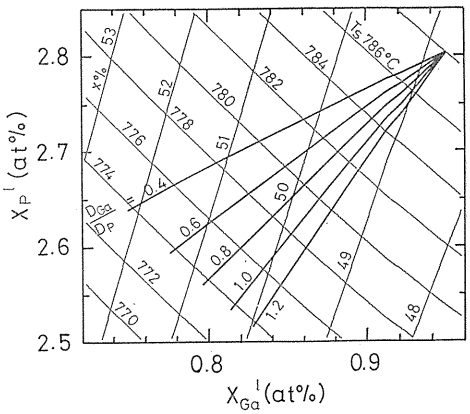

Fig. 5. 2. Growth lines calculated for the ultimate cooling rate at various diffusion coefficient ratio.

growth line at the D_{Ga}/D_P ratio of 0.56 as shown in Fig. 5.2. In the case of step-cooling, the growth lines shift along the isotherm with the growth time. On the other hand, in the case of the supercooling, the growth lines shift along the isotherm at first. Then the growth lines bend and shift to another direction, which is in agreement with the direction of the growth line obtained for the equilibrium-cooling at $C.R.$ of 0.5℃/min, as shown in Fig. 5.1.

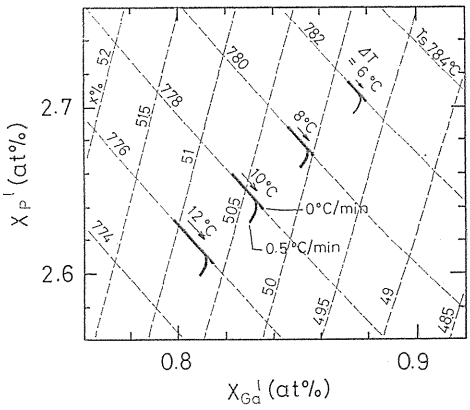

Fig. 5. 3. Growth lines calculated for step-cooling and supercooling at various initial supersaturations.

Thus, the growth lines at the initial growth stage are related to the initial supersaturation but not to the cooling rate. These tendencies are explained by the fact that the gradients of the solute concentration profiles at the interface vary more largely at the initial growth stage because of the presence of the initial supersaturation ΔT, so that when $D_{Ga}=D_P$, the large variation of the diffusion flux ratio J_{Ga}/J_P takes place and shifts the growth line at the initial growth. Therefore, with increasing ΔT, the variation of J_{Ga}/J_P and hence the growth line shift increases.

Figures 5.4 and 5.5 show the variations of In atomic fraction x as a function of the growth time t_g and the layer thickness d for various ΔT's of 4 to 12℃. As shown in Fig. 5.4, at the initial short time less than 5 sec remarkable variations in the solid composition occur. In particular at the initial transient time just after the melt contacts with the substrate the largest variation takes place. These compositional variations are enhanced by increasing ΔT. In addition, the compositional variation occurs at the thin layer of less than 0.3 μm, as shown in Fig. 5.5.

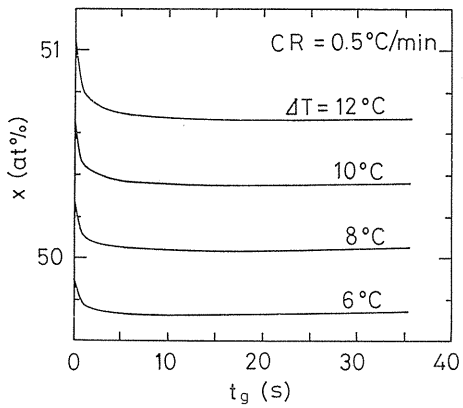

Fig. 5. 4. In atomic fraction x in solid as a function of growth time for various initial supercoolings.

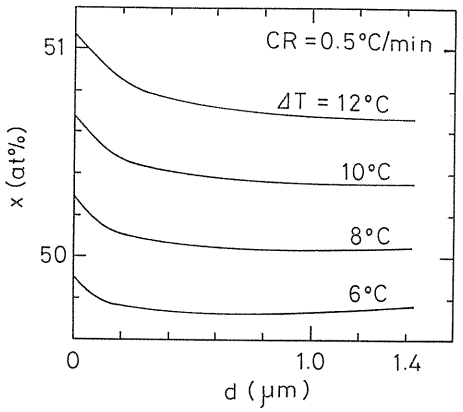

Fig. 5. 5. In atomic fracion x in the solid as a function of the layer thickness for various initial supercoolings.

5. 4. *Discussion*

The experimental results on the compositional variation Δx and the layer thickness d were compared with the theoretical results. The values of D_{Ga} and D_P were determined by fitting the theoretical curves of d vs. t_g and Δx vs. ΔT to the experimental data, as shown later in Figs. 5. 6 and 5. 8. Hence, D_{Ga} and D_P used in the calculation were again taken 1.3×10^{-4} and 2.3×10^{-4} cm^2/s, respectively.

Figure 5. 6 shows the theoretical and experimental variations of d as a function of t_g. Here, ΔT was determined as 6℃ from the difference of T_s and T_g, and $C.R.$ was 0. 5℃/min. The experimental data agree well with the theoretical line. The theoretical d depends on the time as $t_g^{1/2}$, which shows the diffusion limited process.

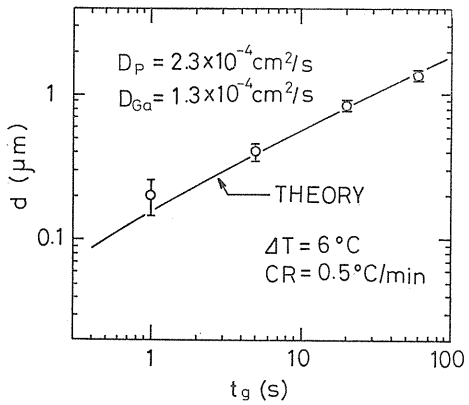

Fig. 5. 6. Thickness of the epitaxial layers as a function of growth time.

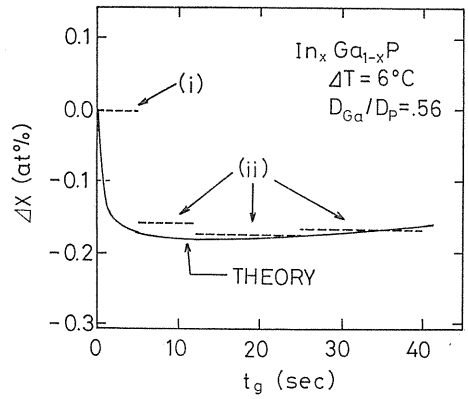

Fig. 5. 7. Compositional variation Δx as a function of the growth time. (i) and (ii) were obtained by the peaks of (i) and (ii) of the X-ray rocking curves shown in Fig. 4. 3, respectively.

Figure 5.7 shows the variation of the solid composition Δx as a function of t_g measured by repeating step-etching of the epitaxial layer grown by the supercooling technique (ΔT=6℃, $C.R.$=0.5℃/min). It is shown that the compositional variation occurs at the initial short stage less than a few seconds, in agreement with the theoretical result.

Figure 5.8 shows the theoretical variation of composition $|\Delta x|$ which occurs at t_g less than 10 sec as a function of T_g or ΔT for various D_{Ga}/D_P's. The value of $|\Delta x|$ increases with increasing ΔT and also with decreasing D_{Ga}/D_P. Here, the equilibrium saturation temperature T_s is estimated to be about 788℃ by extraporating the theoretical curves to the axis of T_g. This value is rather good agreement with T_s of 786℃ which was estimated from the growth temperature dependence of the layer thickness and the surface morphology.[1,2] By fitting the experimental curve with theoretical one, D_{Ga}/D_P is determined as 0.56. When ΔT is less than 8℃, the experimental $|\Delta x|$'s agree well with the theory, but when ΔT is larger than 8℃, $|\Delta x|$'s are smaller than the theory. This fact is attributed to the decrease in the supersaturation dte to the three dimensional nucleation (i.e. homogeneous nucleation) which occurs when ΔT is larger than 8℃.[18]

Next, the compositional variations by experiment for the different ΔT of 4 to 14℃ at $C.R.$ of 0.5℃/min were compared with the theoretical growth lines as shown in Fig. 5.9. The open and closed circles correspond to the solid compositions before and after the variation occurs at the initial transient growth, i.e. the peaks (i) and (ii) in the XRC's, respectively. These two points are plotted along the isotherms because the compositional variations take place at initial short time less than several seconds. Thus the experimental growth lines move from the open circles to the closed circles along the isotherms. These growth lines for ΔT less than 8℃ are in agreement with the theoretical ones. However, in the growth lines for ΔT larger than 8℃, the agreement between the theory and the experiment is poor. This tendency may be related to the three dimensional nucleation in the solution. Because of the consumption of the solutes (ΔX_{Ga}^{l}, ΔX_P^{l}) due to the homogeneous nucleation, the averaged solute concentrations over the melt may shift from the starting point ((s) in Fig. 5.9) to the direction given as $\Delta X_{Ga}^{l}/\Delta X_P^{l}$=

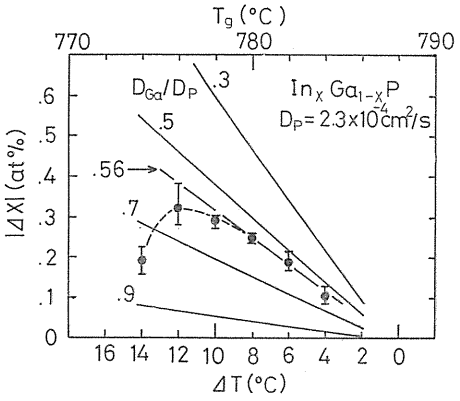

Fig. 5. 8. Compositional variation which occurs less than 10 sec as a function of T_g or ΔT for the various ratios D_{Ga}/D_P.

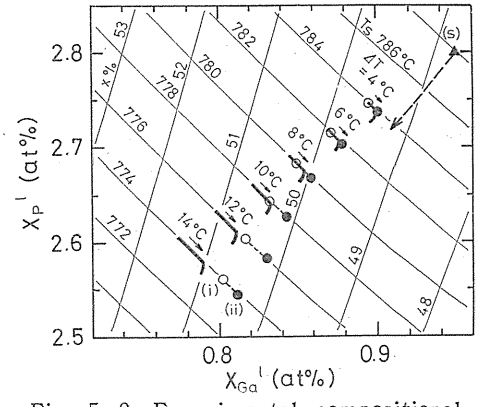

Fig. 5. 9. Experimental compositional variations for various ΔT are compared with the calculated growth lines.

$(1-x)/1.0 \fallingdotseq 1/2$ (the direction of a broken line with an arrow in Fig. 5.9). This direction is in agreement with the direction to which the experimental points for ΔT larger than 8℃ on the phase diagram shift with increasing ΔT. This is in consistent with the decrese in $|\Delta x|$ due to the nucleation for larger ΔT as shown in Fig. 5.8. Furthermore, this ΔT of 8℃ is the same value at which Mukai et al. estimated ΔT from the relation between the layer thickness and the supersaturation.[7]

The theoretical results developed above neglected the effect that the melt is stirred near the solid-melt interface by the motion of the slider when the melt contacts with the substrate. The thickness obtained from the stirred melt is larger than from the unstirred solution, as reported by several authors.[24] This is attributed to the fact that the new solution is supplied to the growing interface by the stir of the melt, so that the larger gradients of the concentration profiles and hence larger diffusion flux are maintained during the stir of the melt. Therefore, the initial solid composition may be kept constant for several seconds by the stir of the melt. In the light of this argument, it is thought that the layer for the peak (i) in XRC is formed at the initial growth.

5. 5. Conclusion

The variation of the solid composition which occurs at the initial transient time in the LPE growth of $In_xGa_{1-x}As_yP_{1-y}$ ($y<0.01$) on GaAs was analysed for the diffusion limited growth model by taking account of the diffusion coefficients. The growth lines on the In-Ga-P phase diagram were calculated by solving simultaneously the diffusion equations of Ga and P, and the phase equilibrium equations. It was found that the theoretical variations of composition explain well the experimental results obtained by the measurements of the X-ray diffractometry. The mechanism of the compositional variation was shown to be based on the large variation of the diffusion flux ratio J_{Ga}/J_P at the initial growth stage in the In melt including two solutes Ga, P with the different diffusion coefficients.

6. Summary

Effects of various growth conditions on surface morphology and compositional non-uniformity of LPE (liquid phase epitaxy) layers of $In_xGa_{1-x}As_yP_{1-y}$ ($y<0.01$) on (100) GaAs were studied. (1) Growth conditions to obtain a smooth and uniform layer was found from the results of change in surface morphology. (2) The interface instability occurring under an undercooling condition in LPE process was studied using analysis of Fourier spectra of the surface morphology. (3) Effects of various growth conditions on compositional non-uniformity of InGaAsP LPE layers on GaAs were investigated by means of the precision X-ray diffractometry. The compositional variation taking place at the initial growth stage during several seconds was found. (4) The variation at the initial stage was analyzed theoretically by "growth lines" on an In-Ga-P phase diagram using the diffusion limited growth model. The growth conditions to decrease the compositional variation was proposed.

Acknowlegements

The authors wish to express their gratitude to Dr. Y. Toyoda with Matsushita Electric Ind. Co. for his help in carrying out the measurements of the double crystal X-ray diffractometry and for valuable discussions and also wish to thank Mr. K. Tomita of Toyota Central Res. and Develop. Laboratories for his useful suggestions. This work was partly supported by a Grant-in-Aid for Scientific Research from the Ministry of Education, Science and Culture of Japan.

References

1) K. Hiramatsu, K. Tomita, N. Sawaki and I. Akasaki: Jpn. J. Appl. Phys. 23 (1984) 68.
2) K. Hiramatsu, S. Tanaka, N. Sawaki and I. Akasaki: Jpn. J. Appl. Phys. 24 (1985) 822.
3) K. Hiramatsu, K. Tomita, N. Sawaki and I. Akasaki: Proc. 16th 1984 Int. Conf. Solid State Devices and Materials, Kobe, Japan, 1984, p. 201.
4) K. Hiramatsu, S. Tanaka, N. Sawaki and I. Akasaki: Jpn. J. Appl. Phys. 24 (1985) 1030.
5) A. Suzuki, H. Kyuragi, S. Matsumura and H. Matsunami: Jpn. J. Appl. Phys. 19 (1980) L 207.
6) S. Mukai, M. Matsuzaki and J. Shimada: Jpn. J. Appl. Phys. 19 (1980) L 505.
7) S. Mukai, M. Matsuzaki and J. Shimada: Jpn. J. Appl. Phys. 20 (1981) 321.
8) S. Mukai, H. Yajima and J. Shimada: Jpn. J. Appl. Phys. 20 (1981) 1001.
9) A. Suzuki, T. Murakami, Y. Kuriyama and H. Matsunami: Jpn. J. Appl. Phys. 21 (1988) L 363.
10) J. J. Hsieh: J. Cryst. Growth 27 (1974) 49.
11) K. Nakajima, S. Yamazaki and K. Akita: J. Cryst. Growth 61 (1983) 535.
12) T. Wada, K. Kubota and T. Ikoma: J. Cryst. Growth 66 (1984) 493.
13) I. M. Lifshitz and V. V. Slyozov: J. Phys. Chem. Solids 19 (1961) 35.
14) C. Wagner: Z. Electrochem. 65 (1961) 581.
15) J. Matsui, K. Onabe, T. Kamejima and I. Hayashi: J. Electrochem. Soc. 126 (1979) 664.
16) P. E. Brunemeier, T. J. Roth, N. Holonyak, Jr. and G. E. Stillman: Appl. Phys. Lett. 43 (1983) 373.
17) K. Oe, Y. Shimoda and K. Sugiyama: Appl. Phys. Lett. 33 (1978) 962.
18) H. Ijuin and S. Gonda: J. Cryst. Growth 23 (1976) 215.
19) I. Crossley and and M. B. Small: J. Cryst. Growth 15 (1972) 268.
20) K. Nakajima, S. Yamazaki and K. Akita: J. Cryst. Growth 56 (1982) 547.
21) M. Ilegems and M. B. Panish: J. Phys. Chem. Solids 35 (1974) 409.
22) G. B. Stringfellnw: J. Cryst. Growth 27 (1974) 21.
23) P. K. Bhattacharya and S. Srinivasa: J. Appl. Phys. 54 (1983) 5090.
24) E. A. Rezek, B. A. Vojak, R. Chin, N. Holonyak, Jr. and E. A. Sammaan: J. Electron. Mater. 10 (1981) 255.